



## Get Clarity On Generics

Cost-Effective CT & MRI Contrast Agents



FRESENIUS  
KABI

WATCH VIDEO

# AJNR

## Corpus Callosum Length by Gestational Age as Evaluated by Fetal MR Imaging

J.H. Harreld, R. Bhore, D.P. Chason and D.M. Twickler

*AJNR Am J Neuroradiol* 2011, 32 (3) 490-494

doi: <https://doi.org/10.3174/ajnr.A2310>

<http://www.ajnr.org/content/32/3/490>

This information is current as  
of August 18, 2025.

## CLINICAL REPORT

J.H. Harreld  
R. Bhore  
D.P. Chason  
D.M. Twickler

# Corpus Callosum Length by Gestational Age as Evaluated by Fetal MR Imaging

**SUMMARY:** Although suspected corpus callosum abnormality is a common indication for fetal MR imaging, biometric data specific to MR imaging are sparse. We sought to characterize growth in corpus callosum length by EGA with fetal MR imaging. Corpus callosum segments were assessed and overall corpus callosum length was measured and plotted against the EGA for 68 anatomically normal fetal brains ranging in EGA from 18.5 to 37.7 weeks, and linear and polynomial regression models were calculated. The body of the corpus callosum was identified in all fetuses, followed in frequency by the splenium (91.2%), genu (85.3%), and rostrum (32.4%). Measurements of corpus callosum length by MR imaging were in agreement with values established by sonography. A second-degree polynomial function was the best fit for callosal length by EGA. Understanding this normal growth pattern may enhance detection of subtle growth abnormalities.

**ABBREVIATIONS:** adj = adjusted; CC = corpus callosum; CI = confidence interval; CNS = central nervous system; EGA = estimated gestational age; HASTE = half-Fourier acquired single-shot turbo spin-echo; SNR = signal-to-noise ratio; SSFSE = single-shot fast spin-echo;  $TE_{eff}$  = effective echo-time

In recent years, MR imaging has become invaluable for evaluation of suspected fetal CNS anomalies. Ultrafast MR images such as HASTE and SSFSE allow imaging of the fetal brain without sedation and with vastly improved delineation of structures not resolvable by sonography. Newer techniques such as parallel imaging, real-time SSFSE, and volumetric sequences promise to continue this trend of improved visualization.<sup>1,2</sup>

Ventriculomegaly and suspected corpus callosal dysgenesis on fetal sonography are frequent indications for MR imaging evaluation because sonographic visualization of the corpus callosum is often limited by suboptimal fetal positioning, maternal body habitus, poor acoustic window due to variations in amniotic fluid volume, and/or limitations imposed by fetal tissue interfaces such as the calvarium.<sup>1</sup> Abnormalities of the corpus callosum rarely occur in isolation.<sup>3</sup> Associated abnormalities, most commonly midline commissural anomalies and cortical malformations, are present in  $\leq 97\%$ .<sup>4,5</sup> Conversely, abnormalities of the corpus callosum are frequently seen in patients previously diagnosed with other CNS abnormalities.<sup>6</sup>

Normative values for corpus callosum length established by sonography<sup>7,8</sup> are not necessarily applicable to fetal MR imaging, given differences in technique, imaging physics, and resolution. Despite the utility of MR imaging in diagnosing callosal and other CNS abnormalities, CNS biometry by MR imaging is a fledgling field. We sought to add to the growing body of literature in this important field by evaluating fetal corpus callosal growth on MR imaging.

## Materials and Methods

Retrospective review of our fetal MR imaging data base from July 2005 through November 2007 yielded 67 fetal subjects having normal CNS anatomy with 68 MR imaging examinations (1 fetus was imaged twice, at 20.2 and 33.2 weeks' gestation) with adequate visualization of the corpus callosum in the midsagittal plane on SSFSE sequences. Gestational age of the fetal subjects, estimated by the combination of early sonographic examination and last menstrual period, ranged from 18.5 to 37.7 weeks (mean, 30.4 weeks). Indications for imaging included suspected neurologic (78%) and non-neurologic (22%) fetal abnormalities; only singleton fetuses with normal CNS anatomy by MR imaging were included in the present study. Fetuses exhibiting any CNS abnormality, including ventriculomegaly, abnormal head circumference, or brain or spinal masses, were excluded. Additional exclusion criteria were multiple gestations, indicators of intrauterine growth restriction such as size/date discrepancies, discordant fetal biometry on sonography or MR imaging, and major organ dysgenesis.

This study met the criteria for exemption from review by our institutional review board and was conducted in compliance with the Health Insurance Portability and Accountability Act. Written informed consent was obtained from each maternal patient. MR imaging was performed on a 1.5T Signa scanner (GE Healthcare, Milwaukee, Wisconsin) without sedation. A surface coil around the maternal pelvis was centered over the fetal region of greatest interest. Following a 15-second 2-plane T2\*-weighted gradient-echo localizer, fetal imaging was performed with the following parameters:  $TE_{eff}$  50–100 ms; FOV, 12–36 cm; matrix,  $256 \times 128$  or  $512 \times 256$ ; bandwidth, 31.2 or 62.5 kHz; NEX, 0.5; section thickness, 3–5 mm. A radiologist monitored each MR imaging acquisition. All fetal brains were imaged in 3 orthogonal planes relative to fetal lie. For fetuses evaluated specifically for CNS abnormalities, sagittal brain images were repeated until images adequate for evaluation of the corpus callosum were obtained.

Images were reviewed on a PC running MagicWeb (Siemens, Erlangen, Germany). Corpus callosum measurements were performed on the best midsagittal images in accordance with sonographic standards, from the anteriormost to posteriormost aspect (Fig 1).

Measurements were acquired by a fetal imager with experience in evaluating >1400 fetal MR imaging studies and by a radiology resi-

Received May 24, 2010; accepted after revision August 1.

From Departments of Radiology (J.H.H., D.P.C., D.M.T.) and Biostatistics (R.B.), University of Texas Southwestern Medical Center at Dallas, Dallas, Texas.

Please address correspondence to Julie H. Harreld, MD, Department of Radiological Sciences, St. Jude Children's Research Hospital, 262 Danny Thomas Pl (MS-220), Memphis, TN 38105-3678; e-mail: julie.harreld@stjude.org or jharreld@yahoo.com

DOI 10.3174/ajnr.A2310

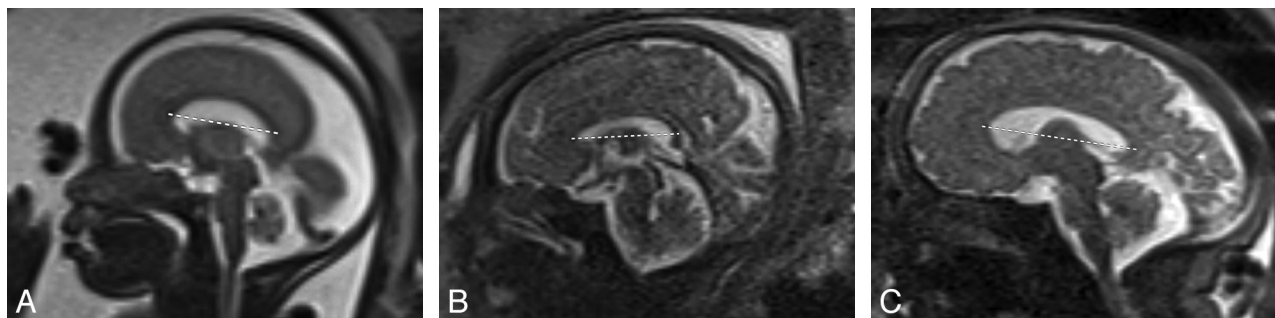


**Fig 1.** Sagittal MR image of the fetal brain ( $TE_{eff}$ , 50–100 ms; NEX, 0.5). Measurement of the corpus callosum from anterior to posterior on fetuses of 25 (A), 33 (B), and 38 (C) weeks' gestational age.

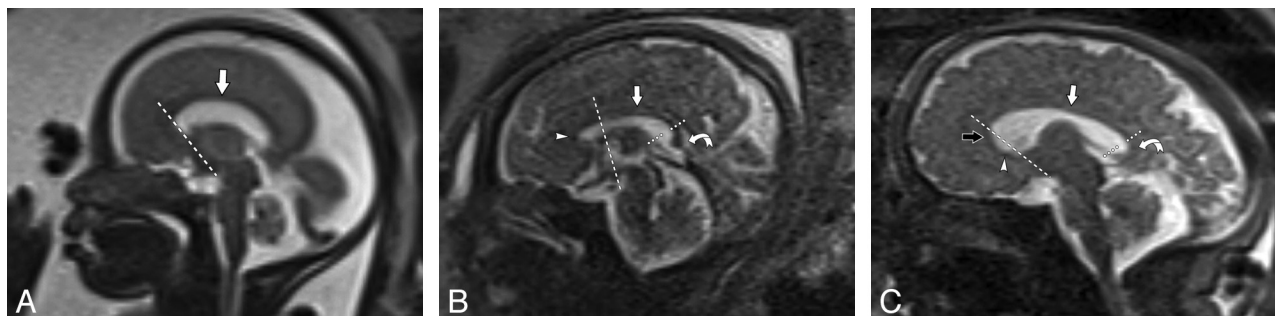


**Fig 2.** Sagittal MR image of the fetal brain ( $TE_{eff}$ , 50–100 ms; NEX, 0.5). Identification of the body (straight arrow), genu (open arrow), splenium (curved arrow), and rostrum (arrowhead) of the fetal corpus callosum at 25 (A), 33 (B), and 38 (C) weeks' gestational age. The genu lies anterior to an approximate line connecting the mamillary bodies (long dotted line), anterior commissure, and corpus callosum.<sup>10</sup> The short dotted line separates the splenium from the body.

dent in the last year of training (after review of the measurement acquisitions in approximately 10 cases) in a blinded fashion. At least 2 measurements were acquired on each image and compared with other available midline images to obtain the most representative measurement. Findings were correlated with gestational age.

Morphologic analysis of the corpus callosum was assessed on mid-sagittal images, with correlation to the coronal and axial planes. Each fetal corpus callosum was assessed for clear visualization of the body, splenium, genu, and rostrum. The body was defined as a low-signal-intensity linear horizontal structure in the expected location of the corpus callosum on the midline sagittal image (Fig 2). The genu was defined as the curved anterior portion of the corpus callosum projecting anterior to an approximate line connecting the mamillary body, anterior commissure, and corpus callosum as described by Kier and Truwit.<sup>9</sup> The rostrum was defined as a beak-shaped segment curving posteriorly or posteroinferiorly from the genu.<sup>10</sup> The splenium was defined as a caudally-oriented or bulbous posterior portion.

Statistical analysis was performed by using SAS, Version 9.1.3 (SAS Institute, Cary, North Carolina). Interobserver agreement was evaluated by a Bland-Altman plot<sup>11</sup> and the Lin concordance correlation coefficient as determined from the identity plot.<sup>12,13</sup> The  $r_c$  examines interobserver measurement reproducibility by measuring the deviation of the fitted relationship of 2 measures from the concordance line (accuracy), and the deviation of each observation from the fitted line (precision). Measurements were considered interchangeable if the Bland-Altman plot demonstrated no clinically significant differences, and  $r_c$  was  $>0.90$ , indicating excellent agreement.

Regression analysis of corpus callosum length versus gestational age was performed by sequential analysis of polynomial fits (linear, quadratic, and cubic) and the logarithmic model. Model assumptions were checked through diagnostics of the residuals, and the best regression fit was chosen on the basis of the highest  $R^2_{adj}$ . Estimated mean

length and 95% CIs were obtained from the best regression fit on the raw data to 1 decimal point for corpus callosum length and EGA.

Regression analysis of published data on fetal corpus callosal length by sonography<sup>7,8</sup> and MR imaging<sup>14,15</sup> was performed for comparison. For direct comparison with published data, we calculated mean corpus callosum length (mm) for gestational age rounded to the nearest integer. An  $F$ -test<sup>16</sup> compared regression models, with  $P < .05$  indicating a statistically significant difference.

The probability of visibility of the splenium, genu, and rostrum was predicted through logistic regression with gestational age as the predictor.

## Results

Although  $r_c$  of 0.92 indicated excellent agreement between experienced and novice imagers (Fig 3), 3 subjects were excluded because the novice observer was unable to confidently measure the corpus callosum length. Bland-Altman analysis (Fig 4) showed a mean difference of 0.27 mm between the 2 observers (95% CI,  $-6.6$ – $7.1$  mm). Because the 2 imagers' observations fell outside the 95% CI, with clinically significant differences between observers, agreement was judged insufficient for interchangeability and expert measurements were used for analysis.

Least squares regression analysis of fetal corpus callosum length ( $n = 68$ ) versus EGA (Fig 5) demonstrated the best fit to be a second-degree polynomial function ( $y = -40.37 + 4.017x - 0.048x^2$ , where  $y$  = corpus callosum length and  $x$  = EGA) as evidenced by  $R^2_{adj}$  ( $R^2_{adj} = 0.828$ ). Normative values of mean corpus callosum length by EGA predicted by this quadratic model are given in the Table.

Regression analysis of published sonography<sup>7,8</sup> and MR imaging<sup>14,15</sup> data similarly demonstrated the second-degree

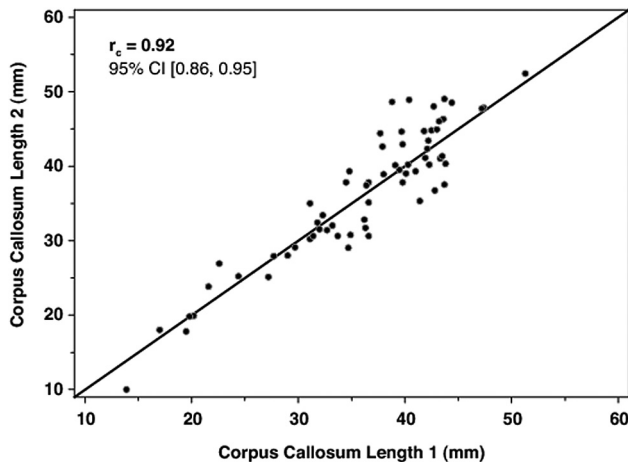


**Fig 3.** Plot of identity demonstrating the correlation of measurements of fetal corpus callosal length between experienced and novice fetal imagers. The  $r_c = 0.92$  suggests excellent correlation between observers.

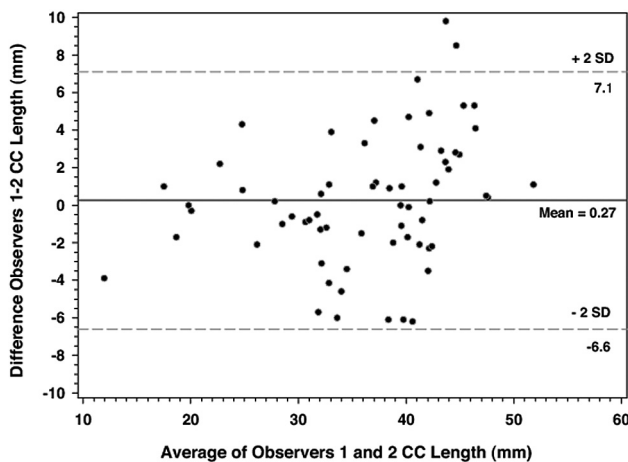


**Fig 4.** Bland-Altman plot of differences between observer measurements of callosal length versus the average of the callosal lengths from 2 observers. The mean difference in measurement between observers was  $0.27 \pm 3.44$  mm.

polynomial to be the best fit ( $R^2_{adj} = 0.910-0.990$ ) (Fig 6). For purpose of direct comparison, regression analysis of our data in terms of average corpus callosum length by gestational week was performed. An  $F$ -test<sup>16</sup> comparing the 5 multiple regression models yielded a  $P$  value of 0.605, implying that the quadratic regression model fits for the 5 studies are statistically similar.

The body of the corpus callosum was identified in all fetal subjects, followed in frequency by the splenium (91.2%), genu (85.3%), and rostrum (32.4%). The earliest visualization of the rostrum was at 20.2 weeks' gestation. In all 22 patients (32%) in whom the rostrum was seen, the body, genu, and splenium were also identified. The probability of segment visualization by gestational age is shown in Fig 7.

## Discussion

Callosal agenesis and dysgenesis are frequently accompanied by, and often herald, other CNS abnormalities.<sup>1,3,5,6</sup> Early identification of callosal dysgenesis can thus be a valuable guide to pregnancy management, delivery, and neonatal care. To this end, there has been great interest and some debate in

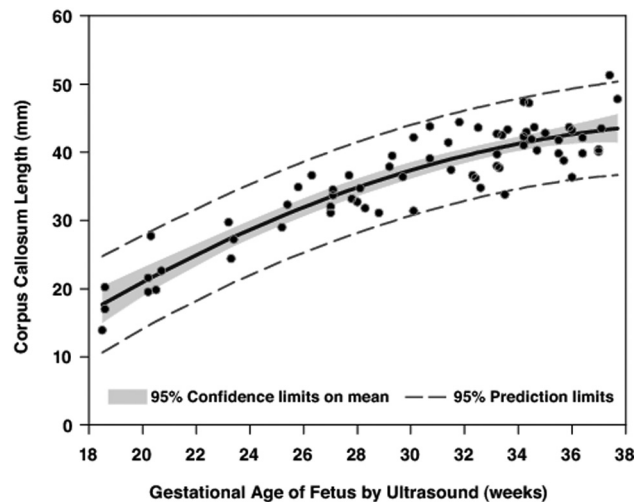


**Fig 5.** Fetal corpus callosal length by gestational age. The line is described by a second-order polynomial  $y = -40.37 + 4.017x - 0.048x^2$ , where  $y$  = corpus callosum length and  $x$  = gestational age.  $R^2_{adj} = 0.828$ . Inner bands show 95% CIs on mean length and surround the line of fit. Outer bands show 95% prediction intervals for individual observations.

the literature regarding the developmental morphology of the corpus callosum and an interest in establishing normative lengths by gestational age. Although normative values of corpus callosum length are well established by sonography, only 1 group<sup>15</sup> has proposed normative values by MR imaging until now.

We demonstrate that despite differences in technology, measurements of corpus callosum length by sonography and MR imaging are statistically equivalent. Additionally, increase in corpus callosum length with gestational age follows a second-degree polynomial function rather than the linear model commonly assumed in the literature. This nonlinear function applies not only to our data but also to other published data<sup>7,8,14,15</sup> and is in keeping with the following observations: 1) Rapid linear growth of the corpus callosum in the second trimester is followed by slower growth in the third,<sup>8</sup> and 2) the initial rostrocaudal linear growth is followed by increasing genuflexion anteriorly.<sup>17</sup> Because the polynomial growth curve reflects both linear growth and folding, examination of the growth curves themselves in individual patients over time may help detect subtle abnormalities of length and morphology as have been identified in entities such as fetal alcohol syndrome.<sup>18</sup> Accurate characterization of the normal growth curve is critical for such analysis.

Although a diagnosis of complete agenesis of the corpus callosum is fairly straightforward, the accurate diagnosis of hypogenesis or dysgenesis requires knowledge of normal development and appearance of the corpus callosum in the fetus. Although this study was not intended as an in-depth review of normal fetal corpus callosal developmental morphology, our data suggest that caution should be applied to the diagnosis of callosal hypogenesis in the fetus. Certain apparent abnormalities such as absence of the rostrum or nonvisualization of the expected flexion of the genu can be normal, depending on gestational age. The rostrum in our cohort was first visualized at 20.2 weeks, correlating to the in-growth of crossing fibers between 20 and 22 weeks.<sup>17</sup> However, the rostrum was visualized in only 44% of fetuses at 37 weeks' EGA, likely due to

Predicted mean corpus callosum length in weeks with 95% CI on the mean and for an individual measurement by gestational age <sup>a</sup>						
EGA (weeks)	No. (total = 68)	Lower 95% CI (Individual) (mm)	Lower 95% CI (of Mean) (mm)	Predicted Mean CC Length (mm)	Upper 95% CI (of mean)	Upper 95% CI (Individual) (mm)
18	3	9.4	13.6	16.5	19.4	23.7
19	— <sup>b</sup>	11.8	16.4	18.8	21.2	25.8
20	5	14.1	18.9	21.0	23.0	27.8
21	— <sup>b</sup>	16.2	21.3	23.0	24.7	29.8
22	— <sup>b</sup>	18.3	23.5	25.0	26.5	31.7
23	3	20.2	25.5	26.9	28.2	33.6
24	— <sup>b</sup>	22.0	27.4	28.7	29.9	35.3
25	3	23.7	29.1	30.3	31.6	37.0
26	1	25.3	30.7	31.9	33.2	38.6
27	6	26.8	32.2	33.4	34.7	40.1
28	4	28.2	33.6	34.8	36.1	41.5
29	3	29.5	34.9	36.1	37.3	42.8
30	4	30.7	36.2	37.4	38.5	44.0
31	3	31.8	37.4	38.5	39.5	45.1
32	4	32.9	38.5	39.5	40.5	46.1
33	7	33.8	39.5	40.4	41.4	47.0
34	8	34.6	40.3	41.3	42.2	47.9
35	5	35.3	40.9	42.0	43.1	48.6
36	4	35.9	41.3	42.6	44.0	49.3
37	5	36.4	41.5	43.2	44.9	49.9

<sup>a</sup> For example, CC length for a fetus of 28 weeks should range from 28.2 to 41.5 mm, with the mean length falling within the range of 33.6–36.1 mm with 95% confidence.

<sup>b</sup>  $n = 0$ ; values are interpolated.

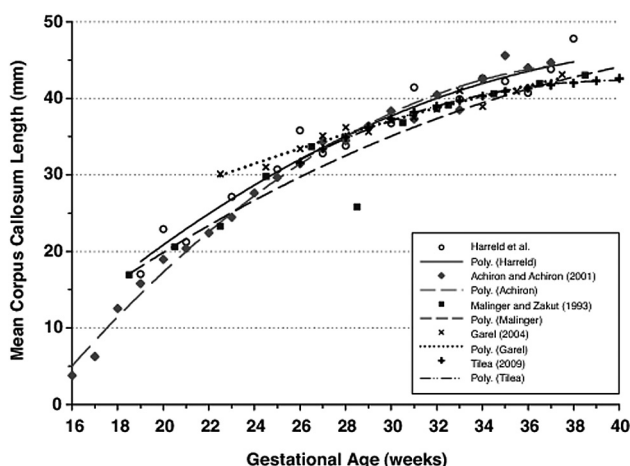


**Fig 6.** Comparative regression analysis of fetal corpus callosal length for data by Harreld et al (this paper) compared with Achiron and Achiron,<sup>7</sup> Maling and Zakut,<sup>8</sup> Garell,<sup>14</sup> and Tilea et al.<sup>15</sup> All data are well described by second-degree polynomial functions, and there is no statistically significant difference among all regression lines ( $P = .605$ ).

technical factors and small size, limitations that should be considered when interpreting fetal MR imaging.

In addition, the body and splenium of the corpus callosum were frequently visualized without a clear morphologic genu, particularly earlier in gestation. The corpus callosum is routinely described as developing from anterior to posterior from genu to body to splenium, with the rostrum developing last. However, postmortem studies describe the formation of the commissural plate at the site of the prospective knee (genu) followed by bidirectional rostrocaudal growth; flexion of the genu actually begins later, around 18 weeks' gestation, and increases to term.<sup>17</sup> The corresponding appearance on fetal MR imaging is that of the corpus callosum developing first in the region of the unflexed anterior body, followed by bidirectional growth and subsequent flexion of the genu.<sup>9</sup> Thus, the

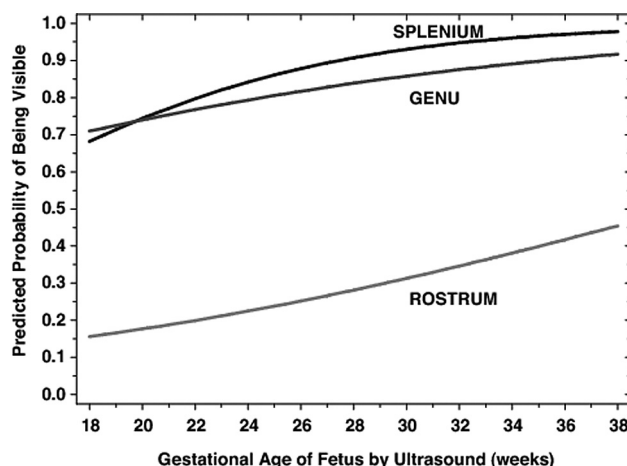


**Fig 7.** Predicted probability of visualization of the splenium, genu, and rostrum of the corpus callosum by gestational age. The callosal body was visualized at all gestational ages imaged.

absence of a discernible flexion may not be abnormal, particularly at early gestational age.

The major limitation of this study is a relatively small sample size. Only a small percentage of fetuses are referred for MR imaging, and though sagittal images of the brain are acquired on all fetuses, only for targeted evaluation of the CNS are they repeated if they are initially inadequate for evaluation of midline structures. Thus many neurologically normal fetuses referred for non-CNS indications were excluded. Although data were sparse for some gestational ages within our data range, the regression model allows interpolation of predicted callosal length within that range without extrapolation of the fitted model.

Although advances in MR imaging technology and the development of SSFSE sequences permit visualization of fetal structures without significant motion artifacts, inherent



trade-offs between resolution and SNR limit visualization of the fetal corpus callosum, which measures just 1.7–4.4 cm. In addition, small degrees of obliquity likely increase the variation of callosal length; osseous attenuation and dependence on fetal lie present similar challenges on sonography. Although 3D MR imaging techniques, such as sampling perfection with application-optimized contrasts by using different flip angle evolutions, would allow reconstruction of a sagittal midline image, these sequences are currently too easily rendered uninterpretable by motion to be practical for fetal imaging. Thus, each fetal MR image should be monitored in real-time by a radiologist to ensure that adequate images are acquired, and these limitations should be considered during image interpretation. Continued advances in MR imaging technology promise further reductions in these limitations.

The low probability of visualization of the rostrum even at an advanced gestational age is problematic because even partial agenesis of the corpus callosum is associated with significant abnormalities. Because the rostrum does not contribute to the length of the corpus callosum, a nomogram of length does not reflect its presence or absence. Therefore, normal corpus callosum length does not imply a normal rostrum. Conversely, nonvisualization of the rostrum at MR imaging even at a late gestational age does not necessarily imply abnormality.

Although we sought to exclude fetuses with any CNS or growth abnormality, it is possible that some of the subjects had unknown syndromes resulting in undetected abnormalities of CNS development that could affect corpus callosum length. This would likely account for only a small number of subjects because 78% were referred for evaluation of the CNS and the CNS was ultimately found to be anatomically normal. Because the antenatal neuroanatomy was normal in these subjects, postnatal imaging of the corpus callosum was not performed. However, agreement of our measurements with values established by sonography and the only other available MR imaging study supports this cohort as being representative of the healthy population.

In summary, we present normative values for corpus callosum length from 18.5–37.7 weeks on fetal MR imaging and demonstrate that despite differences in technology, measurements of corpus callosum length by sonography and MR imaging are statistically equivalent. To the authors' knowledge, this is the first time normative values by MR imaging are presented before 22 weeks. A second-degree polynomial function best describes the fetal corpus callosum growth curve, the ac-

curate characterization of which may be helpful in diagnosis of subtle abnormalities of corpus callosum development. Excellent correlation but suboptimal agreement of measurements by expert and inexperienced observers suggests that fetal MR imaging is best interpreted by experienced fetal or pediatric neuroimagers. Finally, our data suggest that caution be applied to the diagnosis of callosal hypogenesis in the fetus because certain apparent abnormalities such as absence of the rostrum or nonvisualization of the expected flexion of the genu may be normal, depending on gestational age.

## References

1. Glenn OA, Barkovich AJ. **Magnetic resonance imaging of the fetal brain and spine: an increasingly important tool in prenatal diagnosis, part 1.** *AJNR Am J Neuroradiol* 2006;27:1604–11
2. Levine D, Cavazos C, Kazan-Tannus JF, et al. **Evaluation of real-time single-shot fast spin-echo MRI for visualization of the fetal midline corpus callosum and secondary palate.** *AJR Am J Roentgenol* 2006;187:1505–11
3. Glenn OA, Barkovich J. **Magnetic resonance imaging of the fetal brain and spine: an increasingly important tool in prenatal diagnosis, part 2.** *AJNR Am J Neuroradiol* 2006;27:1807–14
4. Hetts SW, Sherr EH, Chao S, et al. **Anomalies of the corpus callosum: an MR analysis of the phenotypic spectrum of associated malformations.** *AJR Am J Roentgenol* 2006;187:1343–48
5. Fratelli N, Papageorgiou AT, Prefumo F, et al. **Outcome of prenatally diagnosed agenesis of the corpus callosum.** *Prenat Diagn* 2007;27:512–17
6. Barkovich AJ, Norman D. **Anomalies of the corpus callosum: correlation with further anomalies of the brain.** *AJR Am J Roentgenol* 1988;151:171–79
7. Achiron R, Achiron A. **Development of the human fetal corpus callosum: a high-resolution, cross-sectional sonographic study.** *Ultrasound Obstet Gynecol* 2001;18:343–47
8. Malinger G, Zakut H. **The corpus callosum: normal fetal development as shown by transvaginal sonography.** *AJR Am J Roentgenol* 1993;161:1041–43
9. Kier EL, Truwit CL. **The normal and abnormal genu of the corpus callosum: an evolutionary, embryologic, anatomic, and MR analysis.** *AJNR Am J Neuroradiol* 1996;17:1631–41
10. Kier EL, Truwit CL. **The lamina rostralis: modification of concepts concerning the anatomy, embryology, and MR appearance of the rostrum of the corpus callosum.** *AJNR Am J Neuroradiol* 1997;18:715–22
11. Bland JM, Altman DG. **Statistical methods for assessing agreement between two methods of clinical measurement.** *Lancet* 1986;1:307–10
12. Lin LI. **A concordance correlation coefficient to evaluate reproducibility.** *Biometrics* 1989;45:255–68
13. Crawford SB, Kosinski AS, Lin HM, et al. **Computer programs for the concordance correlation coefficient.** *Comput Methods Programs Biomed* 2007;88:62–74
14. Garel C. *MR Imaging of the Fetal Brain: Normal Development and Cerebral Pathologies.* New York: Springer-Verlag; 2004
15. Tilea B, Alberti C, Adamsbaum C, et al. **Cerebral biometry in fetal magnetic resonance imaging: new reference data.** *Ultrasound Obstet Gynecol* 2009;33:173–81
16. Zar JH. *Biostatistical analysis.* 4th ed. Upper Saddle River, New Jersey: Prentice Hall; 1999
17. Rakic P, Yakovlev PI. **Development of the corpus callosum and cavum septi in man.** *J Comp Neurol* 1968;132:45–72
18. Astley SJ, Aylward EH, Olson HC, et al. **Magnetic resonance imaging outcomes from a comprehensive magnetic resonance study of children with fetal alcohol spectrum disorders.** *Alcohol Clin Exp Res* 2009;33:1671–89